

Nonmagnetic-Impurity-Induced Antiferromagnetic Long-Range Order in Two-Dimensional Spin-Gapped Heisenberg Antiferromagnet

Chitoshi Yasuda, Synge Todo*, Munehisa Matsumoto, and Hajime Takayama
Institute for Solid State Physics, University of Tokyo, Kashiwa 277-8581, Japan
(January 22, 2001)

Effects of static nonmagnetic impurities on a spin-gapped Heisenberg antiferromagnet on a square lattice are studied by the quantum Monte Carlo method. It is found that the antiferromagnetic long-range order (AF-LRO) appears immediately when a very small amount of nonmagnetic impurities are substituted for magnetic atoms. In a weak dilution, the AF-LRO is mostly carried by localized magnetic moments induced around nonmagnetic impurities with weak effective interactions between them. We observe a clear plateau in the temperature dependence of the effective Curie constant, reflecting the existence of the low-lying excitation modes within the spin singlet-triplet gap.

PACS numbers: 75.10.Jm, 75.10.Nr, 75.40.Cx, 75.40.Mg

The first inorganic spin-Peierls (SP) compound CuGeO₃ [1] exhibits various interesting phenomena inherent to a quasi-one-dimensional (quasi-1D) quantum spin system [2]. The most peculiar one among them is the antiferromagnetic long-range order (AF-LRO) induced by nonmagnetic impurities. When a small amount of Zn or Mg is substituted for Cu, the spin-gapped SP ground state of the pure system changes to a new ground state with the AF-LRO, thereby the lattice dimerization is preserved [3]. It is called the dimerized AF (DAF) state. By the further substitution the lattice dimerization disappears resulting the uniform AF (UAF) state [4]. These transitions also happen when Si is substituted for Ge [5]. We may call the former the site-dilution-induced AF-LRO, while the latter the bond-disorder-induced one. Theoretically these transition phenomena have been attributed to the strong quantum nature of the SP state in a quasi-1D system which is drastically affected by a small amount of nonmagnetic impurities [6].

Associated with the lattice dimerization the intrachain exchange interactions are significantly alternating. Quite interestingly, by the neutron inelastic scattering experiment [3,5], the spin singlet-triplet gap, Δ_p , is observed in the DAF phase as well as in the SP phase, while in the DAF state the low-lying modes within the gap are additionally observed. These results strongly suggest that the higher dimensionality than 1D is another important ingredient of this transition which does not associate vanishing of the spin gap.

In the present work we investigate ground-state transitions in the site-diluted 2D $S = 1/2$ AF Heisenberg (AFH) model by the quantum Monte Carlo (QMC) simulation which can treat the interchain coupling on the equal footing as the intrachain coupling. The lattice degrees of freedom are discarded since we consider that at least the SP-DAF transition is essentially of a magnetic origin. Our QMC simulation on the model reproduces, as we will show below, the SP-DAF transition which is qualitatively in agreement with that observed experimentally. It leads us to the following picture on this transition

similar to the one proposed previously for a spin ladder system by Iino and Imada [7]. Spins on the sites neighboring a site whose spin is removed by dilution organize a spin cluster which is a close resemblance of the edge state in a spin-gapped chain [8]. We call it as a whole an ‘effective spin’. Between the effective spins there exist the effective interactions mediated by spins which are in the dimer (singlet) state. The averaged magnitude of the effective interactions is exponentially small as a function of the degree of dilution. Although they are either ferromagnetic or AF depending on relative positions of the effective spins, the staggered nature with respect to the original lattice is completely preserved, and so the effective spins are antiferromagnetically ordered at $T = 0$.

The quantum spin system of our present interest is described by the Hamiltonian

$$\begin{aligned} \mathcal{H} = & \sum_{i,j} \epsilon_{2i,j} \epsilon_{2i+1,j} \mathbf{S}_{2i,j} \cdot \mathbf{S}_{2i+1,j} \\ & + \alpha \sum_{i,j} \epsilon_{2i+1,j} \epsilon_{2i+2,j} \mathbf{S}_{2i+1,j} \cdot \mathbf{S}_{2i+2,j} \\ & + J' \sum_{i,j} \epsilon_{i,j} \epsilon_{i,j+1} \mathbf{S}_{i,j} \cdot \mathbf{S}_{i,j+1}, \end{aligned} \quad (1)$$

where 1 and α ($0 \leq \alpha \leq 1$) are the intrachain alternating coupling constant, J' (≥ 0) is the interchain AF coupling constant and $\mathbf{S}_{i,j}$ is the quantum spin operator at site (i, j) . Randomly quenched magnetic occupation factors $\{\epsilon_{i,j}\}$ independently take either 1 or 0 with probability $1 - x$ and x , respectively, where x is the concentration of nonmagnetic sites.

In the present work the QMC simulations with the continuous-imaginary-time loop algorithm [9] is carried out on the $S = 1/2$ system on $L \times L$ square lattices with the periodic boundary condition. For diluted systems with $x > 0$ the number of samples averaged over is $100 \sim 700$ depending on x . The staggered magnetization, $M_s(x)$, at zero temperature is evaluated by

$$M_s^2(x) = \lim_{L \rightarrow \infty} \lim_{T \rightarrow 0} \frac{3S_s(L, T, x)}{L^2}, \quad (2)$$

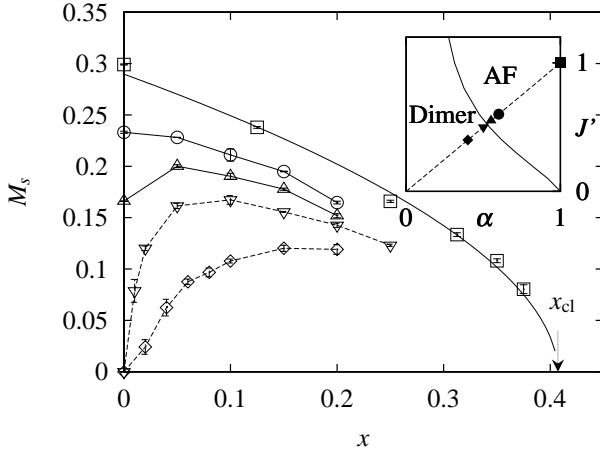


FIG. 1. Concentration dependence of the staggered magnetization at zero temperature for various parameters $\alpha = J' = 1, 0.6, 0.55, 0.5$, and 0.4 in the $\alpha - J'$ phase diagram as inset. Data for $\alpha = J' = 1$ are results in ref. [11] and all lines are guides to eyes. The percolation threshold is also shown as x_{cl} ($\simeq 0.407254$).

where

$$S_s(L, T, x) \equiv \frac{1}{L^2} \sum_{i,j} (-1)^{|r_i - r_j|} \langle S_i^z S_j^z \rangle \quad (3)$$

is the static staggered structure factor. The bracket $\langle \dots \rangle$ in Eq. (3) denotes both the thermal and random averages. The value of $S_s(L, T, x)$ converges to its zero-temperature values at T lower than either a gap due to the finiteness of the system or the intrinsic spin gap. Thus $S_s(L, T, x)$ at low temperatures where its T -dependence becomes not discernible within the error bars is taken as an estimate of $S_s(L, 0, x)$.

First we determine the ground-state phase diagram of the pure system on the $\alpha - J'$ plane. The result is shown in the inset of Fig. 1. The phase boundary between the AF and dimer phases is determined by the finite-size scaling analysis. Except for the critical point $(\alpha, J') = (1, 0)$ the critical exponent of the correlation length associated with the transitions obtained is $0.71(3)$. The value is consistent with that of the 3D classical Heisenberg model [10].

The site-dilution effect has been examined for systems with $\alpha = J'$ indicated in the inset of Fig. 1. The system with $\alpha = J' = 1$ was investigated in details in the previous works [11,12]; the site-dilution simply reduces M_s which exists already in the pure system. For the systems with $\alpha = J' = 0.5$ and 0.4 , on the other hand, M_s , which is zero for $x = 0$, becomes finite even with 1 or 2 % of dilution. This is nothing but the site-dilution-induced AF-LRO, and is a central result of the present work.

Let us begin discussions on our result with the explanation how to extract M_s in Fig. 1. In Fig. 2 the L -dependence of $S_s(L, 0, x)/L^2$ of the system with $\alpha = J' = 0.5$ and $0 \leq x \leq 0.2$ is demonstrated. The data for $x = 0$ are well fitted to $S_s(L, 0, x)/L^2 \propto (1 - \exp(-L/\xi_p))/L^2$.

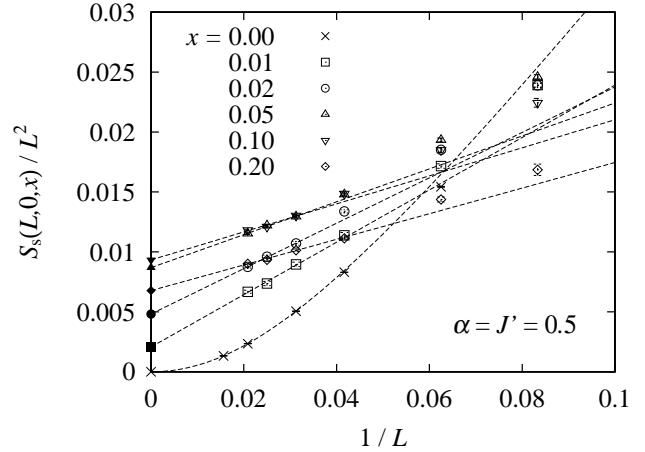


FIG. 2. System-size dependence of $S_s(L, 0, x)/L^2$ in the case of $\alpha = J' = 0.5$. Dashed lines are obtained by the least-squares fitting for the largest three system sizes for each x . The extrapolated values are denoted by solid symbols.

This form is derived by the modified spin-wave theory for a spin-gapped state, where ξ_p is the correlation length. For diluted systems with $x > 0$, on the other hand, M_s is evaluated by fitting the data to $S_s(L, 0, x)/L^2 \simeq M_s^2/3 + a/L$ which is obtained, for example, by the linear spin-wave theory on the state with a finite M_s .

The above-mentioned correlation length of the pure system, ξ_p , is given by $\xi_p = (\xi_p^x \xi_p^y)^{1/2}$ where ξ_p^x and ξ_p^y are the anisotropic correlation lengths. They are estimated from the dynamic staggered correlation function by using the second moment method [13]. Similarly the spin gap, Δ_p , is evaluated from behavior of the function on the imaginary-time axis. We obtain $\xi_p^x = 11.998(9)$, $\xi_p^y = 9.312(10)$ and $\Delta_p = 0.0918(1)$ for $\alpha = J' = 0.5$, and $\xi_p^x = 3.0089(9)$, $\xi_p^y = 2.2097(6)$ and $\Delta_p = 0.32255(3)$ for $\alpha = J' = 0.4$. The nearer to the dimer-AF critical line a system is, the smaller is Δ_p and the larger is ξ_p . For $\alpha = J'$, the quantum phase transition occurs at $\alpha = \alpha_c = 0.52337(3)$.

In order to gain insights into nature of the site-dilution-induced AF-LRO obtained above, we investigate the static local staggered susceptibility defined by

$$\chi_i^s \equiv \beta \sum_j (-1)^{|r_i - r_j|} \langle S_i^z S_j^z \rangle \quad (4)$$

with $\beta = 1/T$. Figure 3 shows the real-space distribution of $\chi_i^s T$ for $\alpha = J' = 0.5$ on a 64×64 lattice from which 30 spins are randomly removed. The temperature, $T = 0.001$, can be regarded as zero temperature for the system with these parameters. The points protruding downwards to zero are on the diluted sites. The peaks of $\chi_i^s T$ appear on the sites connected by a strong bond 1 with these diluted sites. Naturally they are considered to be the contribution of the spins which get rid of the singlet pairing by the dilution. The peaks exhibit a significant spatial extent whose size is given by ξ_p^x and ξ_p^y .

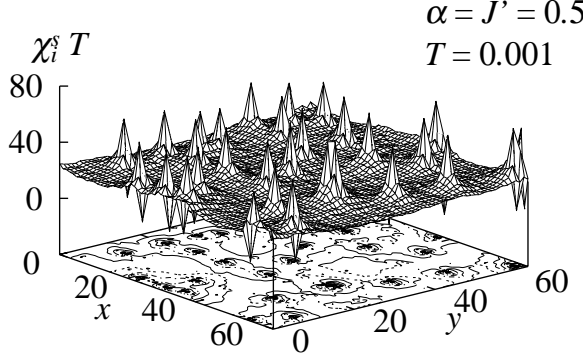


FIG. 3. 3D plot of the static staggered local susceptibility for a fixed configuration of 30 impurities on a 64×64 lattice for $\alpha = J' = 0.5$ at $T = 0.001$. Peaks of magnetic moments appear on sites strongly bonded to the impurity site. Contours are shown in the bottom.

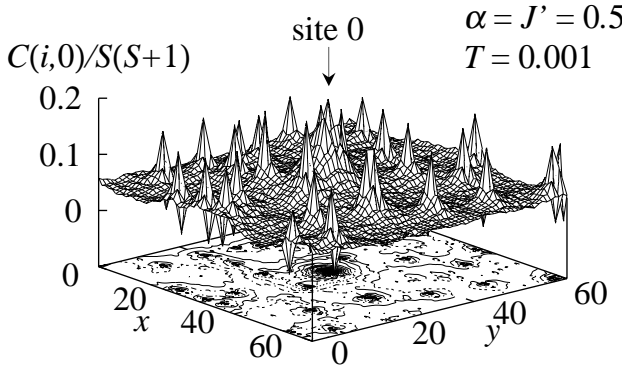


FIG. 4. 3D plot of the staggered correlation function from the peak of an induced magnetic moment on site 0 ($= (31,31)$) for the same impurity configuration as Fig. 3. Correlations between effective spins are stronger than that with other spins.

evaluated above. Figure 3 is thus a direct visualization of the effective spins we have introduced.

From the analogy of the 1D spin-gapped state [14], the exchange coupling between the two effective spins centered at sites m and n is expected to be given by $\tilde{J}_{mn} \propto (-1)^{|r_m - r_n|} \exp[-l(\xi_p^x \xi_p^y)^{-1/2}]$, where $l = |r_m - r_n|$ is the distance between the effective spins. For a sufficiently weak dilution, we can naturally expect that the effective Hamiltonian, $\mathcal{H}_{\text{eff}} = \sum_{\langle m n \rangle} \tilde{J}_{mn} \tilde{\mathbf{S}}_m \cdot \tilde{\mathbf{S}}_n$ well describes magnetic behavior of the effective spins. As we have already pointed out, \tilde{J}_{mn} is considered to completely preserve the staggered nature with respect to the original lattice since the original interactions are all AF with no frustration at all. This is in fact confirmed by Fig. 4 where we demonstrate the static staggered correlation function $C(i,0) = (-1)^{|r_i - r_0|} \langle S_i^z S_0^z \rangle$ with site 0 ($= (31,31)$) being the peak position of an effective spin. The system is the same as that in Fig. 3. At any site i , $C(i,0)$ is positive except for other diluted sites where it is

zero. It peaks at sites of other effective spins with heights almost independent of the distance from site 0, while it stays at a relatively lower value on the sites far from the diluted sites where spins form a local singlet state. Thus Fig. 4 combined with Fig. 3 clearly demonstrates that the site-dilution-induced AF-LRO is mostly carried by the effective spins. Each of them contributes to M_s by the amount proportional to ξ_p^2 , which explains a sharper rise near $x \simeq 0$ of M_s of $\alpha = 0.5$ than that of $\alpha = 0.4$ in Fig. 1. It contributes to the uniform susceptibility, on the other hand, by the amount described as $|\tilde{\mathbf{S}}_m| = 1/2$ [14] as discussed below.

The averaged distance $\langle l \rangle$ between diluted sites is given by $1/\sqrt{x}$. The typical coupling which scales the excitation energy of the spin-wave-like modes is then given by $\langle |\tilde{J}_{mn}| \rangle \propto \exp(-1/\sqrt{x \xi_p^x \xi_p^y})$. It becomes much smaller than Δ_p for a sufficiently small value of x . Thus we can naturally expect the existence of low-lying excitation modes within Δ_p in the DAF state as has been observed by the neutron inelastic experiment [3–5]. We may further conjecture that the experimental fact [3] that the spectrum of the spin-wave-like mode becomes broader for the larger wave number is due to an inhomogeneous broadening, i.e., the AF order of the effective spins is disturbed in the length scale comparable with or less than $\langle l \rangle$.

In the present simulation the existence of the low-lying excitation modes is ascertained by the T -dependence of the effective Curie constant χT which is shown in Fig. 5 for $\alpha = J' = 0.4$ with some x . For $x = 0.01$ a plateau at a height nearly equal to $\chi T = x/4$ in unit of $g^2 \mu_B^2 / k_B$ is clearly seen around $T \sim 0.05$ which is smaller than Δ_p by an order of magnitude. We can attribute the plateau to the Curie law of the effective spins with $|\tilde{\mathbf{S}}_m| = 1/2$ as mentioned above, which are almost freely fluctuating in this range. At lower temperatures than $\langle |\tilde{J}_{mn}| \rangle$, these free effective spins start to correlate with each other.

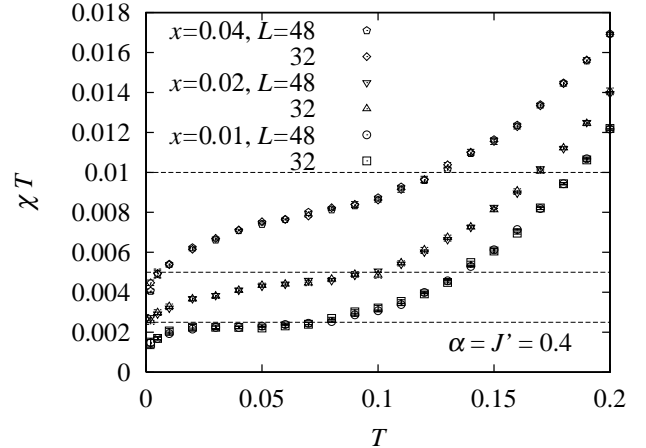


FIG. 5. Temperature dependence of the effective Curie constant for $\alpha = J' = 0.4$. Lines show $\chi T = x/4$ for $x = 0.04, 0.02$, and 0.01 from top.

Then χT decreases to zero as $T \rightarrow 0$. Already for $x = 0.02$, however, the plateau is obscured, indicating that $\langle |\tilde{J}_{mn}| \rangle$ becomes comparable in magnitude with Δ_p . Qualitatively similar features have been also observed experimentally [15]: χ clearly exhibits the Curie law at low temperatures in the system with a sufficiently small value of x .

So far we have shown that the nonmagnetic-impurity-induced AF-LRO observed in the SP compound $\text{Cu}_{1-x}\text{X}_x\text{GeO}_3$ with $\text{X}=\text{Zn}$ or Mg is satisfactorily, though qualitatively, explained by the $S = 1/2$ diluted AFH model described by Eq. (1) with $\alpha = J'$. For a quantitative comparison, the most important quantity is the distance of the ground state of CuGeO_3 from the dimer-AF critical line. It determines ξ_p in the effective coupling $\langle |\tilde{J}_{mn}| \rangle$ which in turn governs quantitatively the x -dependence of various quantities associated with the effective spins. Particularly, $\langle |\tilde{J}_{mn}| \rangle$ scales the Néel temperature of the 3D AF order unless the ground state of the $x = 0$ system is too close to the critical point [16]. These problems are, however, beyond the scope of the present letter.

Let us make one further comment based on the AFH model of Eq. (1). Fixing the interchain coupling, we have compared the x -dependence of the energies of two systems with and without alternation in the intrachain couplings. It is found that the increase in the energy with x of the alternating system is faster than for the non-alternating system. Thus when the lattice energy is taken into consideration, the total energy of the two systems can cross at a certain x . The larger effect of dilution on an alternating system is explained as follows: compared with the non-alternating system, the AF-LRO in an alternating system is more strongly suppressed by quantum fluctuations, and correspondingly the dilution releases this stronger suppression, resulting stronger dependence on x of the energy. This scenario might explain the DAF-UAF phase transition observed experimentally [4].

Lastly it is noted that the $S = 1$ AFH model of Eq. (1) is also confirmed by the QMC simulation to exhibit the site-dilution-induced AF-LRO quite similar to the one studied in the present work [17]. Another interesting problem to be clarified is the bond-disorder induced AF-LRO observed in the CuGeO_3 system [5]. A simple model for this purpose is the bond-diluted AFH model described similarly to Eq. (1). An essentially different feature between the site-diluted and bond-diluted models is expected to exist in a dilute limit. When a stronger bond of magnitude 1 is cut, a pair of free spins appear on two ends of the bond. These two spins suffer from AF interactions proportional to J'^2 which are propagated through the shortest paths between them. Thus in the case that this AF interaction is sufficiently stronger than interactions with free spins created by dilution of different bonds, the

two spins at both ends of a diluted bond again form a singlet pair and cannot contribute to the AF-LRO. This implies a possible existence of a critical concentration x_c below which the AF-LRO does not come out, in contrast to the site-diluted case discussed in the present work. The problem is now under investigation.

In summary, we have argued based on the QMC simulation on the 2D AFH models that nonmagnetic impurities added to a system having the spin-gapped ground state induce effective spins which are strongly correlated. As a consequence there occurs the AF-LRO state which has low-lying excitation states within the spin singlet-triplet gap. The results explain most of the peculiar magnetic phenomena associated with the nonmagnetic-impurity-induced AF-LRO observed in the spin Peierls compound $\text{Cu}_{1-x}\text{X}_x\text{GeO}_3$ with $\text{X}=\text{Zn}$ or Mg .

Most of numerical calculations in the present work have been performed on the SGI 2800 at Institute for Solid State Physics, University of Tokyo. The present work is supported by the “Research for the Future Program” (JSPS-RFTF97P01103) of Japan Society for the Promotion of Science.

* Present address: Theoretical Physics, ETH Zürich, 8093 Zürich, Switzerland.

- [1] M. Hase, I. Terasaki and K. Uchinokura, *Phys. Rev. Lett.* **70**, 3651 (1993).
- [2] O. Kamimura *et al.*, *J. Phys. Soc. Jpn.* **63**, 2467 (1994); O. Fujita *et al.*, *Phys. Rev. Lett.* **74**, 1677 (1995); L. P. Regnault *et al.*, *Phys. Rev. B* **53**, 5579 (1996); M. Nishi, O. Fujita and J. Akimitsu, *Phys. Rev. B* **50**, 6508 (1994).
- [3] M. C. Martin *et al.*, *Phys. Rev. B* **56**, 3173 (1997).
- [4] T. Masuda *et al.*, *Phys. Rev. Lett.* **80**, 4566 (1998).
- [5] L. P. Regnault *et al.*, *Europhys. Lett.* **32**, 579 (1995).
- [6] H. Fukuyama, T. Tanomoto and M. Saito, *J. Phys. Soc. Jpn.* **65**, 1182 (1996).
- [7] Y. Iino and M. Imada, *J. Phys. Soc. Jpn.* **65**, 3728 (1996).
- [8] S. Eggert and I. Affleck, *Phys. Rev. Lett.* **75**, 934 (1995); S. Miyashita and S. Yamamoto, *Phys. Rev. B* **48**, 913 (1993).
- [9] H. G. Evertz, G. Lana and M. Marcu, *Phys. Rev. Lett.* **70**, 875 (1993); B. B. Beard and U.-J. Wiese, *Phys. Rev. Lett.* **77**, 5130 (1996); S. Todo and K. Kato, preprint (cond-mat/9911047).
- [10] P. Peczak, A. M. Ferrenberg and D. P. Landau, *Phys. Rev. B* **43**, 6087 (1991).
- [11] K. Kato *et al.*, *Phys. Rev. Lett.* **84**, 4204 (2000).
- [12] C. Yasuda *et al.*, preprint (cond-mat/0010397).
- [13] F. Cooper, B. Freedman and D. Preston, *Nucl. Phys. B* **210**[FS6], 210 (1982).
- [14] N. Nagaosa *et al.*, *J. Phys. Soc. Jpn.* **65**, 3724 (1996); M. Sigrist and A. Furusaki, *J. Phys. Soc. Jpn.* **65**, 2385 (1996).
- [15] K. Manabe *et al.*, *Phys. Rev. B* **58**, R575 (1998).
- [16] M. Imada and Y. Iino., *J. Phys. Soc. Jpn.* **66**, 568 (1997).
- [17] M. Matsumoto *et al.*, preprint.